

Bachelor Thesis

Writing with a focused electron beam and
decorating with functional molecules

Author:

Joran Böhmer

Supervisors:

Willem F. van Dorp

Jeff Th. M. de Hosson

Materials Science

University of Groningen

Abstract

To understand complex biological systems, we need to observe those small systems. Super-resolution microscopy provides ways for detecting single molecules, while making use of an optical microscope. Fluorophores are attached to nanostructures that start blinking when illuminated with a laser. Various methods are possible to attach fluorophores to the structures. Hereafter the technique called total internal fluorescence microscopy is used to let the fluorophores blink and detect them. This research has shown that passivation of the surface with polyethylene glycol is an essential step in this as well as the use of DNA strings between the surface and the fluorophores. However, future research needs to be done to obtain super-resolved images since the distance between the fluorophores and the surface is too high to be able to detect with total internal fluorescence microscopy.

Contents

1. INTRODUCTION	4
2. THEORETICAL BACKGROUND	5
2.1 Functionalization process	5
2.2 Superresolution microscopy	8
2.3 Controlled blinking behaviour	8
2.4 Total internal reflection fluorescence	9
3. METHODS	11
3.1 Preparation	11
3.2 Functionalization	12
3.3 Fluorescence microscopy	14
4. RESULTS AND DISCUSSION	15
4.1 Optical properties of DLC	15
4.2 Height of the structures	17
4.3 Results and discussion of different labelling methods	17
5. CONCLUSION	22
6. FUTURE RESEARCH	23
7. REFERENCES	23

Abbreviations

AA	Ascorbic acid
APDMES	(3-aminopropyl)dimethylethoxysilane
APTES	(3-aminopropyl)triethoxysilane
B&C	Brightness and contrast
BSA	Bovine Serum Albumin
Cy5	Cyanine 5
DLC	Diamond-like carbon
dsDNA	Double-stranded deoxyribonucleic acid
emCCD	Electron multiplying charged coupling device
FEB	Focused electron beam
FEBID	Focused electron beam induced deposition
FITC	Fluorescein isothiocyanate
FWHM	Full width at half maximum
MV	Methyl viologen
NaHCO₃	Sodium bicarbonate
NHS	N-hydroxy-succinimidyl
PBS	Phosphate buffered saline
PC	Probe current
PEG	Polyethylene glycol
PSF	Point spread function
SEM	Scanning electron microscope
TIRF	Total internal reflection fluorescence
TIRFM	Total internal reflection fluorescence microscopy

1. Introduction

In everyday life there exist many complex biological systems. If we understand the complexities of the systems, we can recreate those systems to use them for our own purposes. Observation plays a big role in the study of such a system. In order to fully understand our system we need to reveal the relevant mechanisms at the single-molecule level. Studying the behaviour of the molecules is the first step to understanding a complex system, which is ultimately needed to design a system for our purposes.

A way of tracing single-molecules is by attaching fluorophores to them after which we localize the structures with an optical microscope. The fluorophores will emit light which is observable by an optical microscope. This technique is called fluorescence microscopy. The downside of this method is that the resolution is limited due to the diffraction of light. The lateral resolution is limited to 200-300 nm whereas the axial resolution is around 500-700 nm [1]. The distance between the molecules to be studied will be far below this range, which makes it impossible to distinguish single-molecules in a bulk of molecules.

The diffraction limit can be surpassed with a technique called super-resolution fluorescence microscopy. In standard optical microscopy the light spot from each fluorophore observed is larger than the distance between the molecules so the individual molecules cannot be identified. If there is a way to switch off all but one fluorophore, then observation of the light spot of a single-molecule is made possible. This light spot will have a Gaussian-like distributed light intensity. Now it is possible to fit a point spread function (PSF) of which the full width at half maximum (FWHM) can be determined. Using this method the lateral resolution is ~25 nm whereas the axial resolution is ~50 nm [1]. If this fitting is done for every fluorophore on the surface, it is possible to reconstruct a super-resolved image [2].

A way to localize single-molecules is to let the fluorophores blink. Blinking is the subsequent switching from the ON and the OFF state. An ideal scenario is one in which there is a low amount of ON states and a high amount of OFF states for it is easiest localizing a single-molecule to fit a PSF to. The blinking of all fluorophores is monitored until all fluorophores have been in the ON state for at least once.

To reduce the complexity and focus only on the technique of reconstructing a super-resolved, the fluorophores will be attached to a surface. Focused electron beam induced deposition (FEBID) is a good method to create high resolution nanostructures on a surface. Its resolution is below the 10 nm range [3]. It is possible to attach functional molecules like fluorophores to the nanostructures [4], making it useful to reconstruct a super-resolved image with super-resolution fluorescence microscopy. This will be the goal of this BSc project.

2. Theoretical background

2.1 Functionalization process

To decorate a surface with functional molecules, a self-assembly method is a convenient way [4]. The basics of the functionalization process consist of three steps (figure 2.1). In a scanning electron microscope (SEM) a precursor gas is released through a needle near the location where it is pleased to deposit the nanostructures. A focused electron beam (FEB) is pointed towards the surface and electrons will react with the gas to form a FEBID. In the next stage the surface will be exposed to a solution with aminosilanes which bind to the nanostructures. Different aminosilanes create different properties for the attachment of the functional molecules.

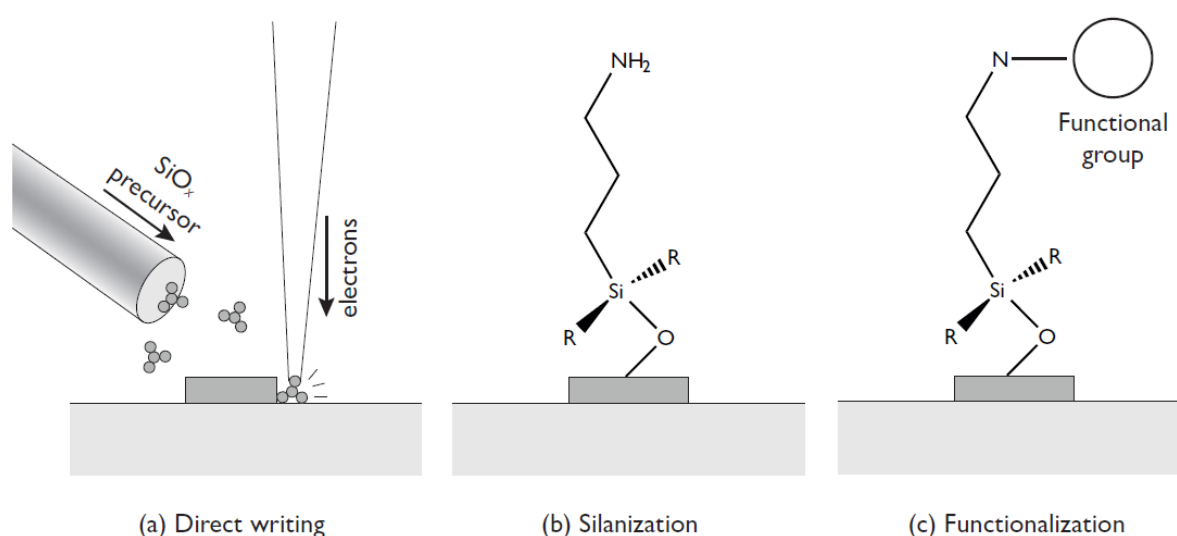


Figure 2.1: The basics of the functionalization process are shown. (a) A silicon oxide gas is exposed to a FEB which creates a deposit on the surface. (b) Silanes from a solution attach to the nanostructures. (c) Functional molecules bind to the silanes. [4]

2.1.1 Focused electron beam induced deposition

FEBID (figure 2.1 (a)) is way of depositing different kinds of solid materials onto a surface in. Some applications FEBID are mask repair for optical lithography [5,6], scanning probe microscopy [7], nanomanipulators [8] and electrical contacts [9]. The solid material that is formed is dependent on the type of precursor gas that is used. In case of the functionalization process a deposition of silicon oxide is used to which the aminosilanes can bind. The gas is injected through a nozzle near the writing location. A beam of electrons then breaks the precursor molecules, leaving behind a silicon oxide deposit on the surface and some non-volatile fragments which are then removed by the vacuum pump in the SEM. The high resolution of this technique makes it very useful for this research where we try to construct a method to observe samples in the smallest detail.

2.1.2 Silanization process

In the silanization process (figure 2.1 (b)) aminosilanes are attached to the newly made nanostructures to create a link between the structures and the functional molecules. The sample surfaces are drowned into a solution of silanes for some time until a layer is created. The aminosilanes consist of a group that can be attached to the silicon oxide and an amine tail to which a functional group can be bonded.

The silanes (3-aminopropyl)triethoxysilane (APTES) [10, 11, 12] and (3-aminopropyl)dimethylethoxysilane (APDMES) [13] have shown to be useful for this specific research (figure 2.2). The difference between the two is that APTES has three functional groups whereas APDMES only has one. Those functional groups can attach to the silicon oxide on the sample surface, but also to other silanes. When APDMES binds to another APDMES silane, the bonded silanes form couples and lose their function. An APTES silane however will polymerize with the other silanes and that polymer can still bind to the nanostructures. This is not preferable since it is hard to regulate the amount of silane that will be bonded to the surface when there are long chains of polymers in the solution.

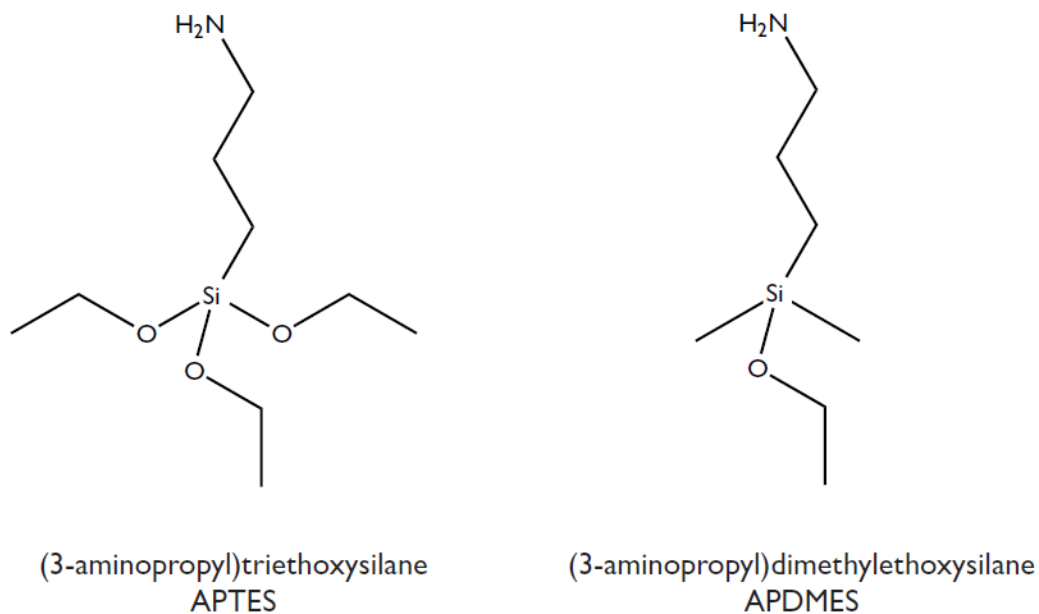


Figure 2.2: The molecular structures of APTES and APDMES.

2.1.3 Functional molecules

Since observation is key in this experiment fluorophores will be used as functional molecules, because they're easily observed in an optical microscope. There is a large selection of fluorophores from which to choose as functional molecule for the experiment. Three of them are worth comparing: fluorescein isothiocyanate (FITC), ATTO655 and cyanine 5 (Cy5). The molecules need to be attached with an N-hydroxy-succinimidyl (NHS) group to let them bind to the silane.

2.1.3.1 FITC

FITC reacts with the silane at such high speed that it is regularly referred to as click chemistry. It is susceptible to photobleaching and losing some of its light intensity via neighbouring molecules or substrates [15]. Photobleaching is a process where the fluorophore will be destroyed through a photochemical reaction. Another big drawback of FITC is that its blinking behaviour can not be controlled by chemicals which makes it a bad contestant for super-resolution blink-microscopy. It is more useful as a quick check-up to see if previous parts of the experiment worked out well.

2.1.3.2 ATTO655

The blinking behaviour of ATTO655 can be controlled with chemicals. Besides that it stays in the ON state for a very short amount of time when blinking [15] which makes it easier to study single-molecules. Also its stability against photobleaching is much higher [16] making it able to observe for a longer period of time.

2.1.3.3 Cy5

Compared to ATTO655, Cy5 has a somewhat less great stability against photobleaching [16] and it also stays in its ON state for a longer period of time when blinking [15]. Same as with ATTO655, the blinking behaviour of Cy5 can be controlled with chemicals.

2.1.4 Specific versus unspecific labelling

There are two ways a fluorophore can attach to the surface: specific and unspecific. With specific labelling the fluorophore undergoes a covalent bonding, making use of its functional group. That functional group will react with its counterpart, which is already attached to the nanostructures, to make a new strong bonding. This doesn't always go as planned. On the other hand the fluorophore can also be attracted to the surface via electrostatic forces, unspecific binding. As a consequence the fluorophores will also "bind" to the background surface, but that's not even the only undesired effect. The fluorophore will also be really close to the surface. When this happens it interchanges energy with the surface making it impossible to control whether a fluorophore will be in its ON or OFF state (2.3 Controlled blinking behaviour).

To increase specificity of the labelling one can passivize the surface with Bovine Serum Albumin (BSA) or polyethylene glycol (PEG). BSA is attracted to the surface via van der Waals forces. This is called physisorption. Physisorption causes the BSA to probably stick everywhere on the surface. It does however seem to be somewhat more attracted to charged material like the nanostructures. PEG undergoes a covalent bonding with all parts of the surface that have been silanized before, which causes the fluorophores to probably bind more specific than BSA. After passivizing a surface, a linker like neutravidin needs to be added to act as a linker between the fluorophore and the BSA or PEG. Also the functional molecule Biotin-NHS needs to be added to the BSA or PEG and the fluorophore. It binds specific and rapid with neutravidin [15], which causes rapid functionalization of the surface.

2.2 Superresolution microscopy

Due to the diffraction of light the resolution of the fluorophores is limited. To achieve higher resolution the molecules need to blink. That way it is possible to observe single-molecules. Figure 2.3 (a) illustrates the image of a single-molecule seen through an optical microscope. It consists of a certain amount of blocks and each block sends a certain amount of photons towards the camera giving them a certain light intensity. The light intensity has to have some Gaussian distributed function. A computer can not only determine the FWHM value, but also give an eight times smaller area of where the fluorophore should be (figure 2.3 (b)).

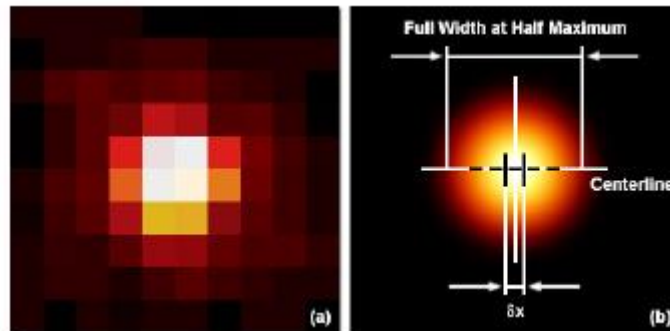


Figure 2.3: Image of a single-molecule [17]. (a) Image after recording data from the microscope, the raw image. (b) Image after a Gaussian fit from a computer.

Last step is to determine the FWHM value and it is easy to give a pretty exact location of where the molecule should be. Repeating this for other single-molecules can give a superresolved image of some drawing with the SEM (figure 2.4).

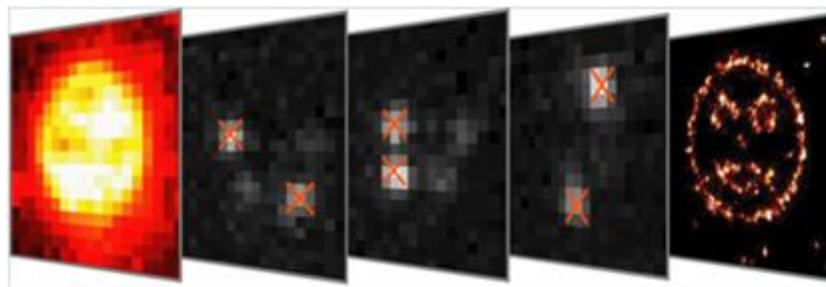


Figure 2.4: An illustration of the procedure from superresolution microscopy [18].

2.3 Controlled blinking behaviour

The behaviour of ATTO655 is described by a model including three energy states (figure 2.5): S_0 , S_1 and T_1 . The ground state and first excited state, S_0 and S_1 , are both singlet states and T_1 is a triplet state. Excitation from the S_0 to the S_1 state happens under the influence of light. This can be done by using a laser. By increasing the laser power the fluorophore makes its cycles faster, but photobleaching will occur more [18]. Switching from the S_1 state to the S_0 states happens under emission of some photons which are detected by a camera. Due to intersystem crossing the fluorophore will turn from the S_1 state to the T_1 state. Intersystem crossing is the switching between electronic states with a different spin arrangement. No

particles are emitted during the transition. By transferring energy to the surface it will turn to its ground state again. These cycles happen at such high speed that photons are emitted almost constantly.

Under the influence of reductants and oxidizers it is possible to take the fluorophore to the OFF state. A reductant can make the fluorophore turn from the S_1 or T_1 state to the F^{*-} state. This state has a long lifetime and only a reaction with oxygen can make the fluorophore turn back to its ground state. Playing with concentrations of reductants and oxygen can vary the fraction of ON to OFF states. Ascorbic acid (AA) can be used as a reductant whereas methyl viologen (MV) can be used as an oxidizer [19,20].

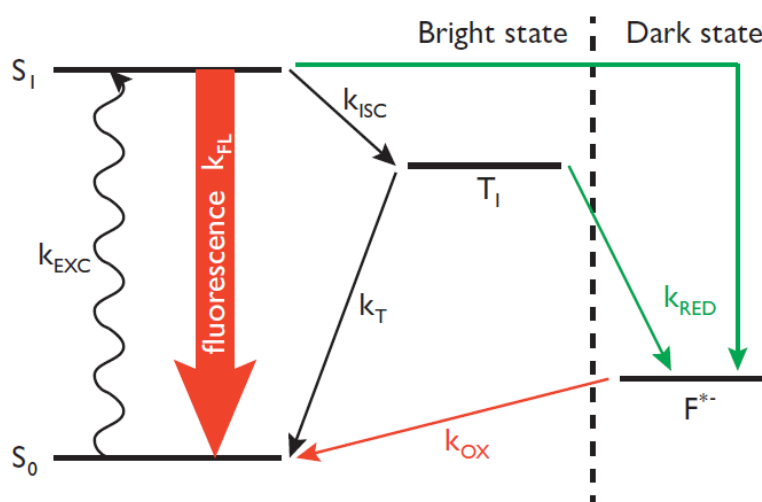


Figure 2.5: An energy state model of the fluorophore ATTO655. The states on the left hand side are short-lived states whereas the lifetime of the F^{*-} state is long. The actual fluorescence is caused by the switching from the S_1 to the S_0 state. [21]

2.4 Total internal reflection fluorescence

The single-molecule superresolution microscopy technique that is used requires a method to suppress background noise of fluorescence. In order to achieve a better signal-to-noise ratio, total internal reflection fluorescence microscopy (TIRFM) is used. Total internal reflection fluorescence (TIRF) provides a way of selectively exciting fluorophores that are within some small region above the surface [22].

A small part of the sample surface is illuminated with a laser. The solution above the cover slide has a smaller refractive index than the cover slide itself. The light is sent in at an angle greater than the critical angle of refraction given by Snell's law, causing all the incident light to be internally reflected in the cover slide (figure 2.6). Above the plane of reflection an electromagnetic field arises, the evanescent field [23]. This happens only when all of the incident light is reflected by the plane. The effective penetration depth of the evanescent waves is approximately 100 nm. Beyond 100 nm the intensity of the evanescent field becomes too low, because of the exponential decay of the intensity of the evanescent field. The fluorophores that are stimulated by the energy of the first 100 nm of the evanescent field will excite to the first state. This is the region where the nanostructures were built.

TIRF is also a wide-field technique, which means that it is applicable to multiple molecules at the same time.

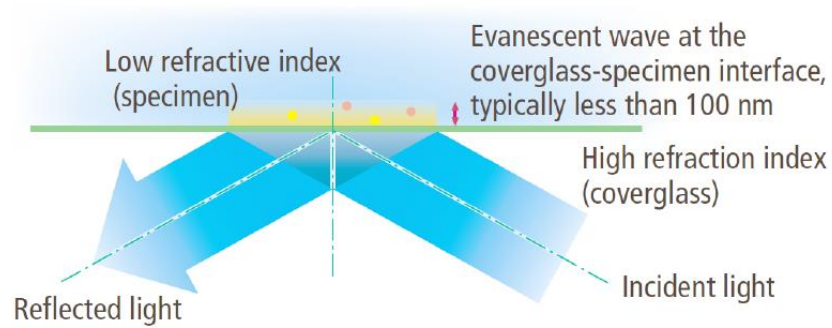


Figure 2.6: An illustration of TIRF [24]. Evanescent waves perpendicular to the surface are generated with an effective range of about 100 nm. The fluorophores in that region will be excited.

3. Methods

3.1 Preparation

First the glass cover slides are being cleaned. This is a five-step process in which each step a different solution is used for cleaning. After each step the cover slides are rinsed with Milli-Q water and put in the next solution. The cover slides are inserted in a coplin jar filled with 150 mL of the following solutions in exactly that order and then put in a sonication bath for 15 minutes. After the last step the cover slides are thoroughly dried.

- Helmanex at 60°C
- Acetone
- Ethanol
- Methanol
- KOH

After this the cover slides are coated with about 50 nm of diamond-like carbon (DLC) coating carried out in a Teer UDP400/4 closed-field unbalanced magnetron sputtering system.

The writing of the FEBID structures is done on a TESCAN Lyra dual beam system. The following settings were used when writing the structures:

- Probe current (PC) of 5.
- Dwell time of 1 μ s.

Two different drawings are made with the SEM: one with blocks (figure 3.1) and one with lines (figure 3.2). The drawings are too small to find back under the optical microscope. That's why a dashed line is etched into the coating with a focused ion beam (FIB) starting from a recognizable feature near the edge of the surface towards the structures. The beam shoots an array of gallium ions that damage the coating and reveal the glass underneath, the same material of which the nanostructures are made.

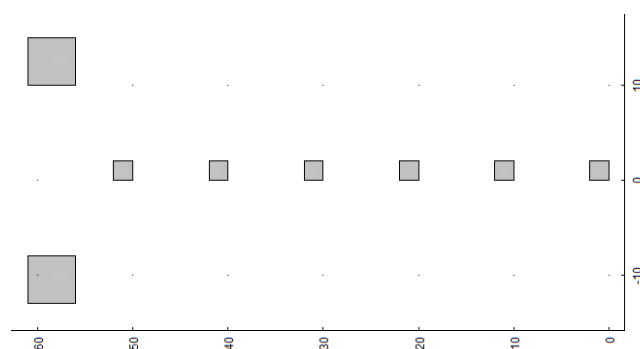


Figure 3.1: The geometry of the block structures. The smaller blocks have dimensions 2x2 μ m and the larger blocks have 5x5 μ m. The small blocks are separated 8 μ m from each other. The accelerating voltage of the field emission electron gun is 5 keV. The number of scans is 10k which results in structures of about 50 nm high. A pitch of 60 nm is used.

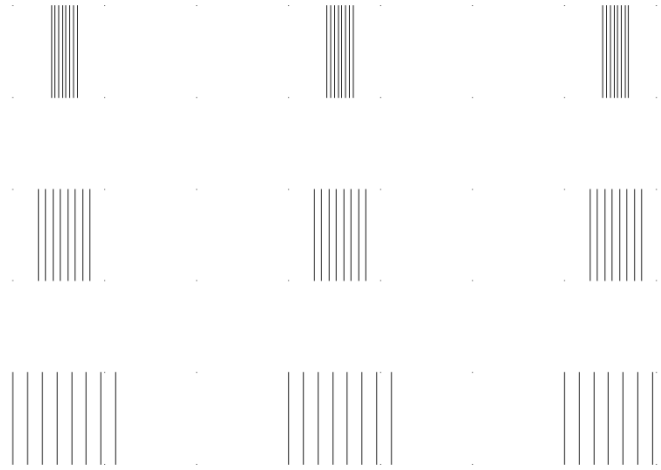


Figure 3.2: The geometry of the line structures. Each set consists of eight lines of 5 μm long. In the third row they're separated by 0.8 μm , in the second row by 0.4 μm and in the first row by 0.2 μm . The accelerating voltage of the field emission gun is 30 keV. In the first column the number of scans is 8k, in the second column it is 16k and in the third column it is 32k. A pitch of 4.5 nm is used.

3.2 Functionalization

Four different methods are used to find the best way to functionalize the nanostructures (figure 3.2). For the silanization APDMES is used, because the polymerization of APTES is unwanted. In one step (figure 3.2 (d)) the silanization and passivation of the surface is combined by using PEG-silane.

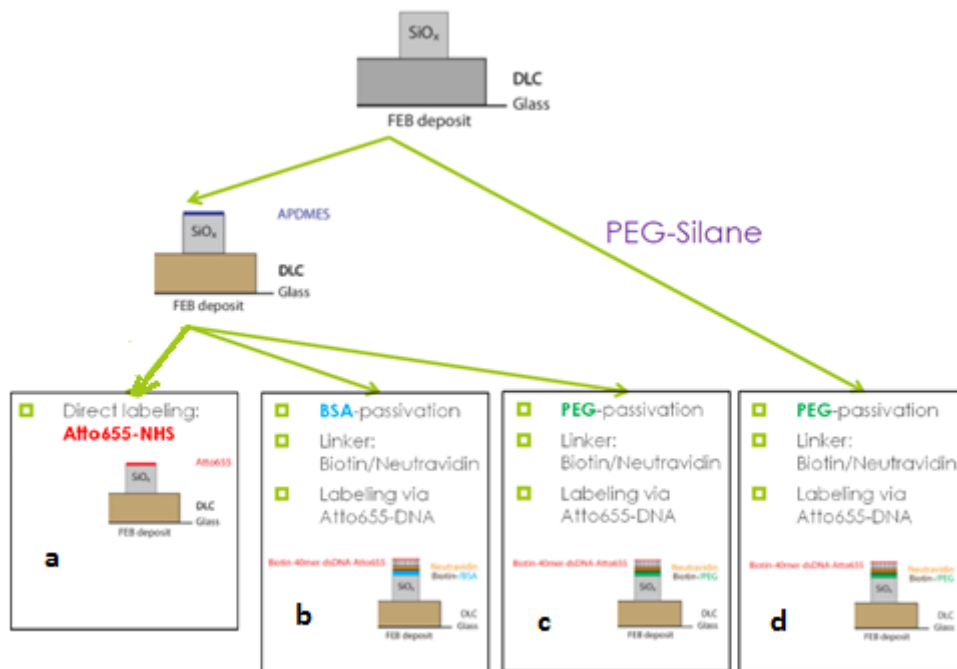


Figure 3.2: An illustration of the four different processes: (a) direct labelling, (b) BSA passivation, (c) PEG passivation, (d) PEG-silanization.

3.2.1 Silanization

For the methods illustrated in figure 3.2 (a),(b),(c) the first step is to silanize the surface via the following procedure:

- Clean the coplin jar 2 times with toluene.
- Add 25 ml of toluene to the jar.
- Heat the jar to 65-70°C in a water or oil bath.
- Mix the toluene with 250 µL of APDMES.
- Put the jar in a sonication bath for half a minute.
- Add the cover slides to the coplin jar and incubate them for 10 minutes at 65°C.
- Rinse the cover slides 3 times with toluene, ethanol and Milli-Q water in this order.
- Store the cover slides in Milli-Q water.

3.2.2 Direct labelling

After silanization, follow the steps below for direct labelling. ATTO655-NHS is used as functional molecule since its blinking behaviour is controllable and it has better properties than Cy5-NHS.

- Make a buffer of 100 mM NaHCO₃ in 60 mL of Milli-Q water.
- Add 500 µL DMSO to 10 nmol ATTO655-NHS giving a 20 µM solution.
- Vortex the solution and take $\frac{1}{200}$ of it to add to 20 mL of the NaHCO₃ buffer giving a 100 nM solution.
- Incubate the cover slides for 10 minutes.
- Rinse the cover slides 10 times with Milli-Q water.
- Store the cover slides in Milli-Q water.

3.2.3 BSA passivation

The silanized surface gets BSA passivation and biotinylation which are described below:

- Add 62.5 mg of BSA to 20 ml of phosphate buffered saline (PBS).
- Add 0.5 mg of BSA-biotin to the solution.
- Incubate the cover slides for 12 hours at room temperature.
- Rinse the cover slides 10 times with Milli-Q water.

After that, the passivized surface is labelled with DNA:

- Incubate the cover slides with 1nM double-stranded DNA (dsDNA) 11/12 for 1 minute.
- Rinse the slides 3 times with PBS.
- Incubate the slides with 0.2 mg/mL neutravidin for 10 minutes.
- Rinse the slides 3 times with PBS.

- Incubate the slides with the dsDNA 11/12 again for different amounts of time. Start with a few minutes and watch every now and then to check if the structures become visible. If not, incubate longer.

3.2.4 PEG passivation

After silanizing the surface, it gets PEGylated:

- Make a 100 mM NaHCO₃ buffer with a pH of 8.
- Add 120 mg of PEG-5000-NHS to 20 mL of the buffer.
- Add 20 mg of Biotin-PEG-5000-NHS to the solution.
- Incubate the cover slides for 12 hours at room temperature.
- Follow the second part of instructions from 3.2.3 (DNA labelling).

3.2.4 PEG silanization

In the process of 3.2.1, the APDMES is replaced by Biotin-PEG-Silane. Follow the instructions of this process. After that follow the second part of instructions from 3.2.3 (DNA labelling).

3.3 Fluorescence microscopy

TIRFM is done using a custom-made microscope based on an Olympus X71 body. A 643 nm Coherent Cube 640-100X laser is used to excite the fluorophores. A Hamatsu electron multiplying charged coupling device (emCCD) camera is used for detecting photons emitted due to fluorescence. A laser power of 140 mW is used with a time interval of 20 to 30 ms.

A silicon gasket is fit on top of the functionalized cover slides. After that a solution of 3 μ M AA and 3 μ M MV in PBS is added in the gasket. There is made sure that no oxygen is present when closing up the gasket with another clean cover slide.

4. Results and discussion

4.1 Optical properties of DLC

When working in TIRF it is useful to know how the DLC coating itself reacts to the light. If it is too hard to observe the nanostructures on our sample, it could have more reasons than only the use of a wrong labelling method. That's why the absorption, transmission and fluorescence properties of the DLC coated cover slides are tested. These properties are compared to the regular cleaned cover slides.

In figure 4.1 the results of absorption and transmission are displayed, which are acquired from a spectrometer. The laser being used with TIRFM has a wavelength of 637 nm so the only relevant optical properties are at a wavelength of 637 nm.

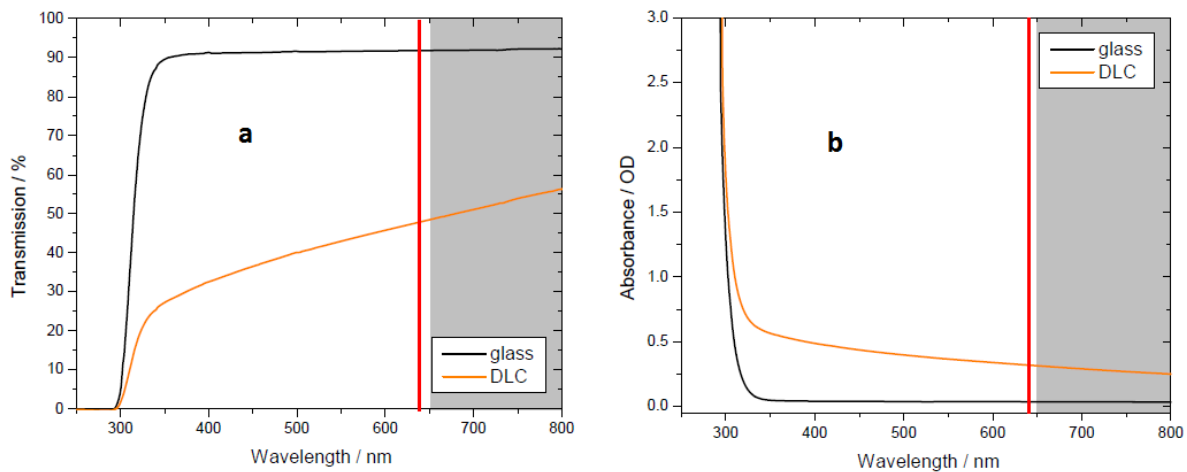


Figure 4.1: (a) Transmission in percentage of incoming light and (b) absorbance properties of DLC coated cover slides. The point of interest is at 637 nm.

We find a transmittance of about 0.5 at the point of interest. Compared to the regular glass, this change in transmittance is caused mainly due to the higher absorbance. From this it is concluded that the DLC coating shows little reflectivity. These properties of the DLC cause a lower excitation power above the DLC coating. Therefore it could be that less fluorophores can be excited from the ground state.

A second issue could be that the DLC has fluorescent properties of itself. The coated cover slides are put in a fluorometer at an angle of 45 degrees towards the incoming light. The light is sent in at two different wavelengths and the registered spectra are compared (figure 4.2).

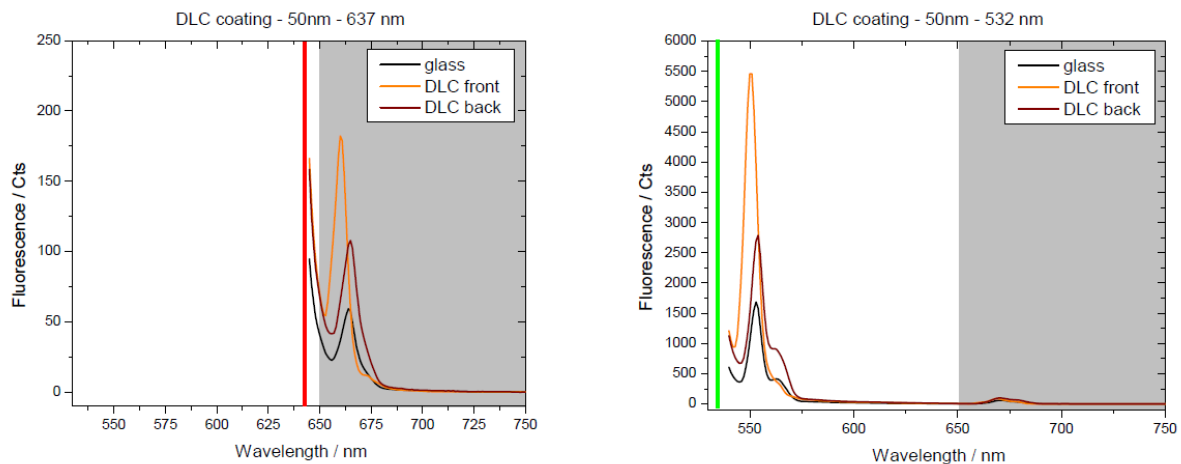


Figure 4.2: The registered light spectra from the fluorometer. Light of two different wavelengths is used: 637 nm and 532 nm.

The comparison of the two spectra indicates the incoming light is Raman scattered, an event that shows similarities with fluorescence [25]. Raman scattering is the inelastic scattering of photons causing photons to be sent back with different wavelengths. This essentially also happens with fluorescence, but it differs from fluorescence as fluorescence can only happen at certain specific wavelengths of the incoming light while Raman scattering can occur at every wavelength. A fluorescence peak is fixed at a certain wavelength while Raman peaks have a constant separation from the excitation frequency. Raman scattering is dependent on the angle at which the incoming light hits the surface. In these tests the cover slides were placed at an angle of 45° towards the incoming light. In a scenario where the angle is 0° the Raman scattering won't occur.

The intensity of the Raman peaks are also compared to the fluorescence of ATTO655 (figure 4.3). This image shows that the Raman peaks are higher than the fluorescence of ATTO655, which means that the fluorescence is overwhelmed by the Raman scattering. However, when observing the nanostructures in TIRF the incident angle of light is 0° . At this angle the Raman scattering ceases to exist, which causes no further complications in TIRFM.

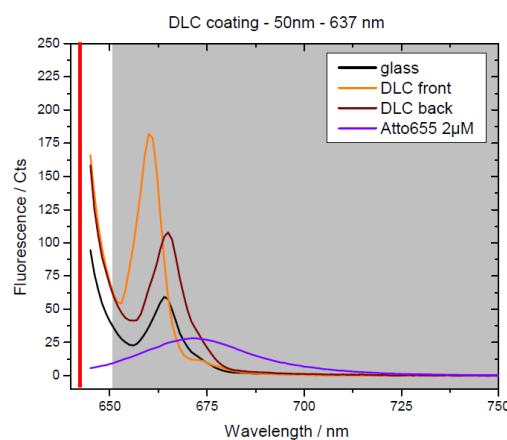


Figure 4.3: The Raman peaks of the DLC are displayed in contrast to glass and a $2\mu\text{M}$ solution of ATTO655.

4.2 Height of the structures

The height of the FEBID structures is important to know, because TIRFM is functional typically to a height of 100 nm. Most of the fluorophores that are above this region won't be excited by the energy of the evanescent wave since this energy will be too low. An estimation of the height of the structures has been made (figure 4.4).

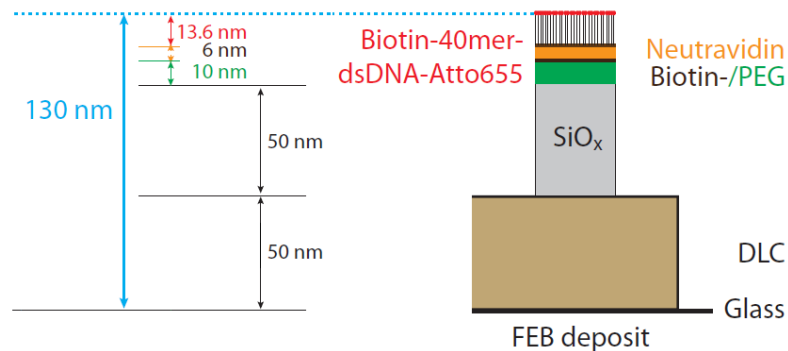


Figure 4.4: An estimation of the height of the FEBID block structures. A stacking of DLC coating (50 nm), silicon oxide (50 nm), PEG (10 nm), neutravidin (6 nm) and dsDNA-ATTO655 (13.6 nm).

For the amount of time the cover slides are left in the magnetron sputter depositor, the slides are left with a coating of 50 nm. With the used settings of the SEM (3.1 Preparation) for the blocks and 10k of scans, a FEBID structure will be made of about 50 nm. The height of the line structures are harder to predict since all scans don't exactly stack on top of each other, but also deposit some silicon oxide next to the arranged lines. So isn't only dependent on the number of scans, but also the distance between the lines. The chemicals altogether add another estimated 30 nm on top of the structures.

The height of 30 nm of chemicals above the structures is needed for successfully controlling the blinking behaviour of the fluorophores. Without the long strings of DNA the fluorophores will interchange energy with the surface and this will mess up the fluorescence. The height of the silicon oxide can be controlled by the number of scans made with the SEM and the height of the DLC coating can be controlled by the time the cover slides are left in the magnetron sputter depositor. However, the DLC coating could crack when it gets thinner since there already are signs of lesser strength at the sides of the cover slides. The height of silicon oxide can be played with to change the height of the structures, but it is expected that it won't distribute evenly onto the selected parts of the surface.

4.3 Results and discussion of different labelling methods

At first we observed the structures in bright field and TIRF without silanizing or functionalizing the structure. The structures are slightly visible in bright field (figure 4.5 (a)) and invisible in TIRF as expected (figure 4.5 (b)). There are no fluorophores that can be excited by the evanescent waves from TIRFM giving the camera no photons to detect.

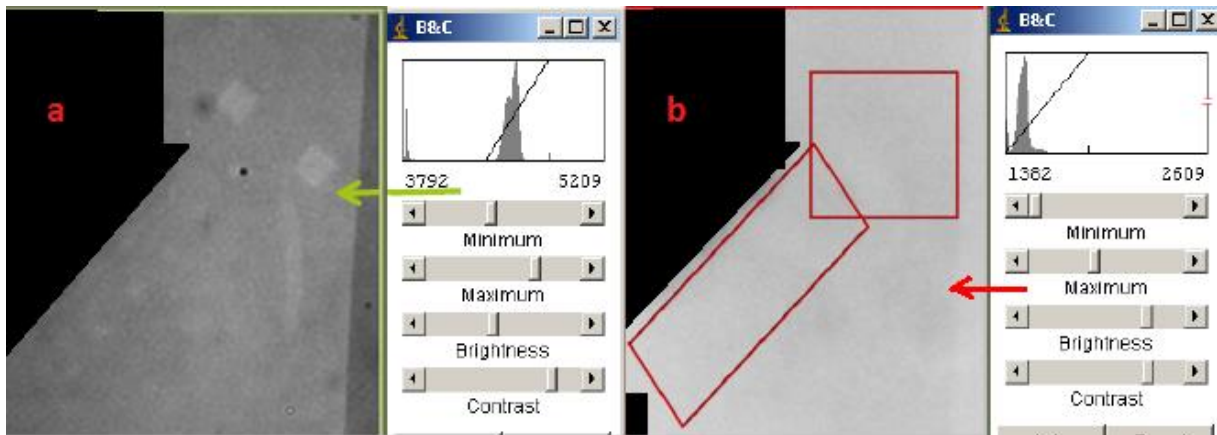


Figure 4.5: Untreated nanostructures in (a) bright field and (b) TIRF accompanied with the used brightness and contrast (B&C) settings.

4.3.1 Direct labelling

Following the method illustrated in figure 4.6 (a), the structures are labelled with ATTO655-NHS and observed in TIRF (figure 4.6 (b)).

The sample seems to show specific labelling, because none of the background of the sample is fluorescent. However, it was impossible to control the blinking behaviour with AA and MV. This means that the ATTO655 was too close to the surface, making it possible for the fluorophore to interchange energy with the surface. This way the fluorophore uncontrollably switches between its ground and excited state. AA or MV won't make any difference in this process. The fluorophores need to have a greater distance from the surface to exclude the interchange of energy with the surface.

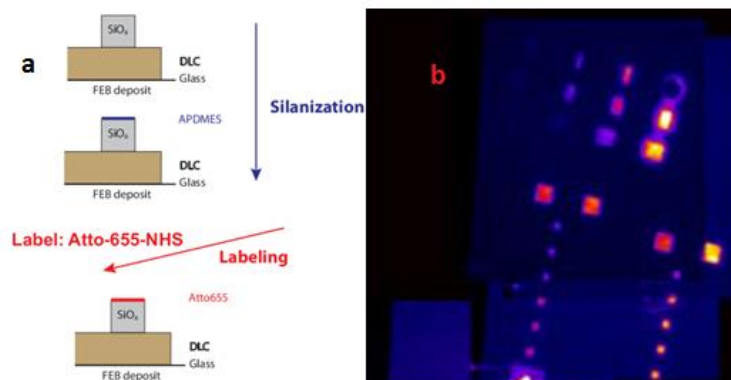


Figure 4.6: (a) The schematics of the method used. (b) The sample seen in TIRF seems to show specific labelling.

An interesting property of the image is the brightness of the structures. For the line structures it varies heavily depending on the number of scans and distance of separation between the lines. In the third column of lines the light intensity is much higher than the that of the square structures. This is explained by the fact that the fluorophores don't only attach to the top of the structures, but also to the sides since the APDMES binds to all silicon

oxide. As the lines get closer to each other, the surface area of the silicon oxide per square unit becomes higher. As the surface area increases, the number of fluorophores per square unit also increases which is the cause for the emission of a higher amount of photons in that area. This explains the increased light intensity.

The upper right set of lines has turned into a crater which seems to not be fluorescent at all. It is yet to be examined what might be the cause of this crater and what it actually exists of. The feature has been seen seldom and appears to exist only when the number of scans become really high whereas the distance separating the lines becomes small. Also, the circumstances under which the craters happen to exist are unnecessary for this research.

4.3.2 BSA passivation

Following the method illustrated in figure 4.7 (a), the surface is passivized with BSA before labelling and observed in TIRF (figure 4.7 (b)). It is seen that the line structures are hardly labelled. BSA has different way of binding to the surface than PEG and it is plausible that it is also stuck to the rest of the surface.

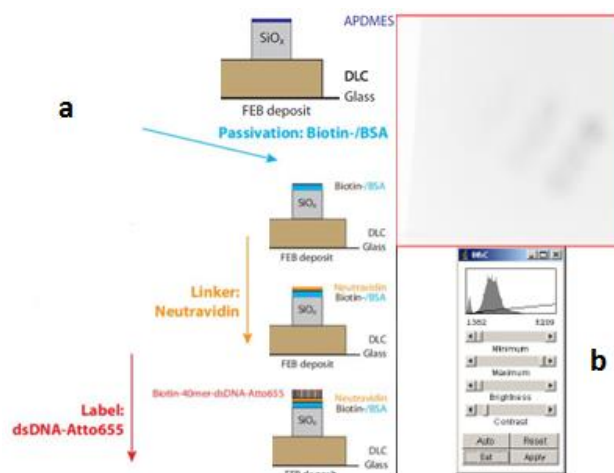


Figure 4.7: (a) Schematics of the method used. (b) The colours of this image are inverted. The sample seen in TIRF hardly shows any labelling of the line structures.

To confirm that the BSA also stuck to the rest of the surface, the surface is observed at less height (figure 4.8). Here we see the surface after only three minutes of incubation time, which is a relatively short incubation time compared to that of PEG passivation for example (4.3.3 PEG passivation). The dashed lines are FIB lines used to retrace the FEBID nanostructures. Although it seems the BSA is more likely to stick to the glass, the lines aren't completely passivized after three minutes, which should imply that a longer incubation time is needed. However the surface is already too contaminated with BSA to which the neutravidin and ATTO655 will bind. As a result the entire surface is left fluorescent. A different approach is needed to successfully passivize the surface.

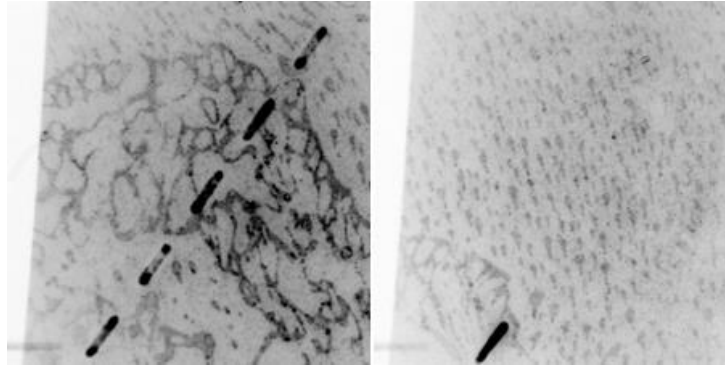


Figure 4.8: The surface of the sample is observed in TIRF after three minutes of incubation in BSA. The colours of the images are inverted. All that is black, except for the dashed lines, is contamination of the surface with BSA. The dashed lines are etched into the coating with a FIB revealing the glass underneath to which the BSA is more likely to stick.

4.3.3 PEG passivation

Following the method illustrated in figure 4.9 (a), the surface is passivized with PEG before labelling and observed in TIRF (figure 4.9 (b,c)). We used two different PEG incubation times, ten and thirty minutes, to be able to give an estimation of time needed for a proper passivation of the surface. It is expected that after some time the PEG may be able to stick to the DLC coating also, but a short incubation time may not entirely cover the structures.

With ten minutes of incubation time, the background of the surface isn't passivized and the FIB line is. The FIB line is labelled entirely with a controllable blinking behaviour which is the goal of this research. However the FEBID line pattern is only slightly visible and has negligible intensity compared to the FIB line. When increasing the incubation time, an undesired side-effect contaminates the background surface. The intensity of the line pattern is slightly increased, but still too low compared to intensity of the FIB line.

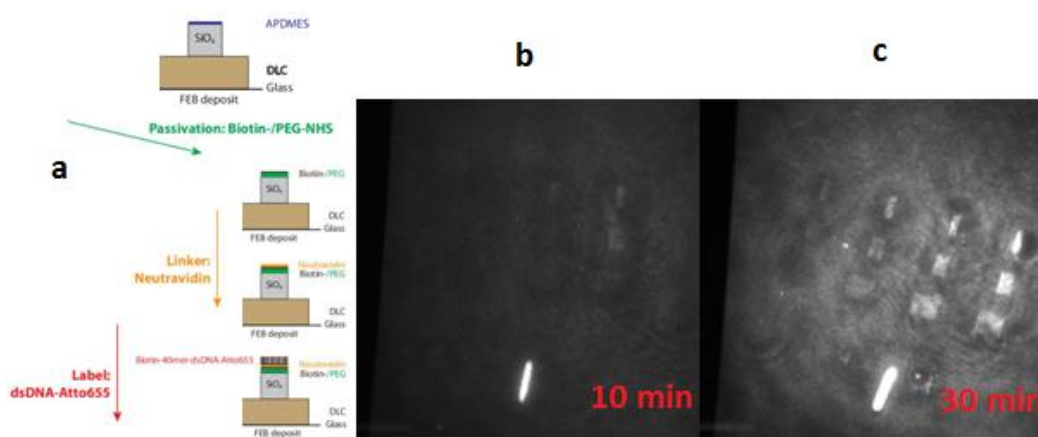


Figure 4.9: (a) Schematics of the method used. (b) An image of the FEBID line pattern incubated for ten minutes in PEG. The FIB line is nicely and specifically labelled, however the line pattern seems to need a longer incubation time. (c) The same image after thirty minutes of incubation. We see some fluorescence on the background surface, caused by bad surface passivation as a consequence of the longer incubation time.

An incubation time of ten minutes seems to be just fine, at least for specifically labelling the FIB line. An increase of the incubation time doesn't solve the problem of detecting the line pattern so there needs to be another explanation for the difference in intensity comparing the FIB line and line pattern. As shown in 4.2, the height of the structures is probably the reason for the low intensity of the line pattern. The method used for functionalizing the structures is probably the correct approach since it works for the FIB line. However the nanostructures need to be lowered somehow.

4.3.4 PEG silanization

Following the method illustrated in figure 4.10 (a), the surface is silanized with PEG-silane, which combines the silanization and passivation process. The method is very similar to PEG passivation (4.3.3 PEG passivation) and also two different incubation times are used to find out the time needed for proper surface passivation.

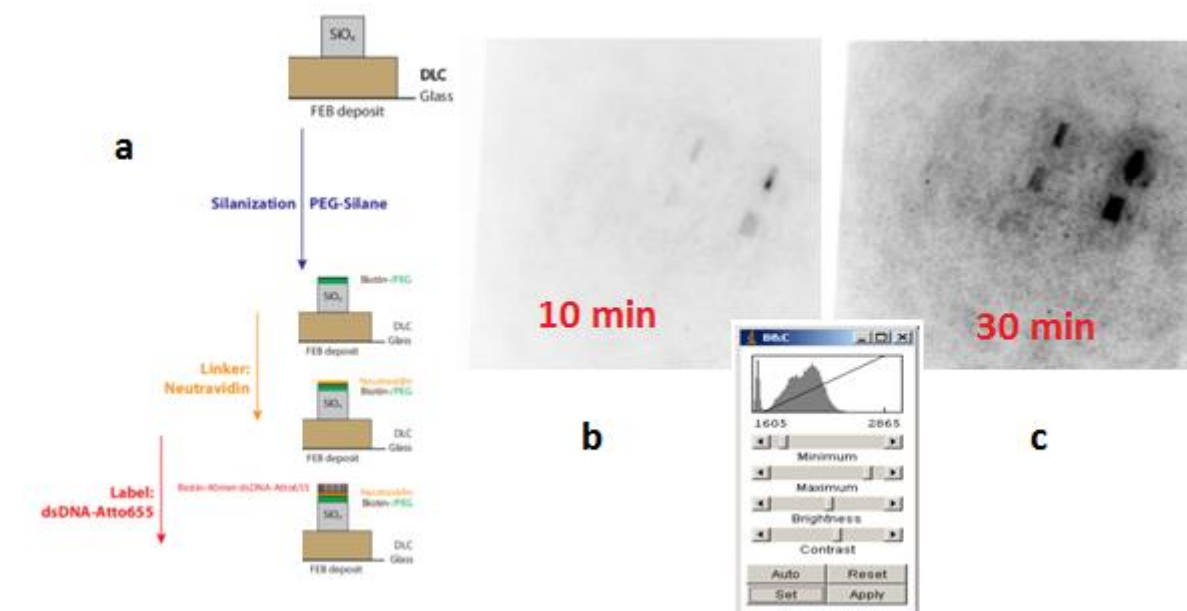


Figure 4.10: (a) Schematics of the method used. (b,c) The colours in these images have been inverted. (b) The FEBID structures seen in TIRF after 10 minutes of incubation with PEG-silane. (c) The same image after 30 minutes of incubation time. The image shows similar effects as figure 4.9 (b,c).

The results obtained through PEG silanization are very similar to PEG passivation. This was also expected since the structures are topped with the same building pieces needed for the functionalization. As with PEG passivation the incubation time of 10 minutes provides excellent passivation of the surface whereas an incubation of 30 minutes messes up the surface passivation. In the first case (figure 4.10 (b)) the image hardly shows any labelling. It is assumed that this has to do with the same reason as with the PEG passivation. The height of the structures exceeds the effective range in TIRFM. There's only one minor advantage with respect to the PEG passivation process and that is that PEG silanization is less time consuming.

5. Conclusion

The tests made for the absorbance and transmittance of the DLC coating show that the absorbance is higher, while the reflectivity is low. Lower excitation power above the DLC coating was expected, but with the laser power being used it gave no trouble. Fluorescent properties of the DLC coating are also measured and something other than fluorescence is noticed while doing the research. The wavelengths of the peaks detected with the fluorometer shift with almost the same amount as the wavelength of the incoming light shifts. This indicates the DLC coating is dealing with Raman scattering. Detecting the Raman scattering in the fluorometer was made possible due to the fact the incoming light was sent in at an angle of 45° . Raman scattering is angle dependent and while it is detectable at an angle of 45° , it ceases to exist at an angle of 0° . This is the angle of the incoming light used in TIRFM so the Raman scattering will be of no importance in the further research.

The height of the structures has been estimated to be at around 130 nm which is about 30 nm higher than the effective region of TIRFM. Only a very small amount of fluorophores will get enough energy from the evanescent wave to turn to the excited state. It is expected that the structures will be hard to detect due to this and the height needs to be lowered.

No single method of functionalization provided an excellent job for detecting the fluorophores in TIRF. However, there were two methods that showed themselves to be of no use in the research: direct labelling and BSA passivation before labelling.

Via the direct labelling method we noticed the blinking behaviour was uncontrollable. This is caused by the small distance between the fluorophore and the surface. This causes an interchange of energy between the fluorophore and the surface which makes the fluorophore switch uncontrollably between its ground and excited state. DNA strings are needed to increase the distance from the surface as well as passivation of the surface to increase the specificity of the labelling.

The BSA was used to cover the structures to increase the specificity of the labelling, but the BSA also stuck to the rest of the surface. The BSA provided bad passivation of the surface so a different chemical is needed for passivizing the surface.

Both the PEG passivation and PEG silanization methods showed to be good methods to functionalize the FIB lines, but the FEBID structures were hardly visible in TIRF. The estimated height of the structures is 130 nm, which is outside the effective range of TIRFM. This is the reason of the low light intensity of the structures. The methods used provide good functionalization, but the structures need to be lowered.

6. Future research

The research hasn't given the appropriate ways of detecting the fluorophores attached to the FEBID structures, which is needed to successfully reconstruct a super-resolved image. In future research we will try to etch parts of the coating away to lower the entire silicon oxide structures. Different numbers of scans will be used with a FIB to obtain multiple terraces of different heights to find the optimal height for observing the structures in TIRF.

7. References

- [1] B. Huang, M. Bates, X. Zhuang, Annual review of biochemistry **78**, 993-1016 (2009)
- [2] S. van de Linde et al., Nature protocols **6**, 991 (2011)
- [3] W.F. van Dorp et al., Nanotechnology **22**, 505303 (2011)
- [4] W. Slingenbergh et al., ACS Nano **6**, 9214 (2012)
- [5] T. Liang, E. Frendberg, B. Lieberman, A. Stivers, Journal of Vacuum Science & Technology B **23**, 3101 (2005)
- [6] K. Edinger et al., Journal of Vacuum Science & Technology B **22**, 2902 (2008)
- [7] J.D. Beard, S.N. Gordeev, Nanotechnology **22**, 175303 (2011)
- [8] P. Bøggild, T.M. Hansen, C. Tanasa, F. Grey, Nanotechnology **12**, 331 (2001)
- [9] S. Bauerdick, A. Linden, C. Stampfer, T. Helbling, C. Hierold, Journal of Vacuum Science & Technology B **24**, 3144 (2006)
- [10] E. T. Vandenberg et al., Journal of colloid and interface science **147**, 103 (1991)
- [11] J. A. Howarter and J. P. Youngblood, Langmuir **22**, 11142 (2006)
- [12] R. M. Pasternack, S. Rivillon Amy, and Y. J. Chabal, Langmuir **24**, 12963 (2008)
- [13] F. Zhang et al., Langmuir **26**, 14648 (2010)
- [14] L. White and C. Tripp, Journal of colloid and interface science **232**, 400 (2000)
- [15] B. Visser, Master thesis: Focused electron beam induced nanostructures for the calibration of Superresolution Blink-Microscopy, 1-108 (2013)
- [16] Q. Zheng, S. Jockusch, Z. Zhou, S.C. Blanchard, Photochemistry and Photobiology **10**, 12204 (2013)
- [17] Education in microscopy and digital imaging: <http://zeiss-campus.magnet.fsu.edu/articles/superresolution/palm/practicalaspects.html>

- [18] T. Cordes et al., Nano letters **10**, 645-651 (2010)
- [19] I.H. Stein, S. Capone, J.H. Smit, F. Baumann, T. Cordes, P. Tinnefeld, ChemPhysChem **13**, 931937 (2012)
- [20] J. Vogelsang et al., ChemPhysChem **11**, 24752490 (2010)
- [21] T. Cordes, J. Vogelsang, and P. Tinnefeld, Journal of the American Chemical Society **131**, 5018 (2009)
- [22] D. Axelrod, The Journal of Cell Biology **89**, 141-145 (1981)
- [23] D. Axelrod, Traffic **2**, 764-774 (2001)
- [24] S. Denham, D. Cutchey, TIRF microscopy: High contrast imaging of surface events, Nikon Instruments (2008)
- [25] E. Plötz et al., Journal of Material Chemistry, DOI: 10.1039/c3tb21763a (2014)